Visible-Light-Induced Controlled Radical Polymerization of Methacrylates Mediated by Pillared-Layer Metal-Organic Framework

Journal:	*Green Chemistry*
Manuscript ID	GC-ART-11-2015-002620.R1
Article Type:	Paper
Date Submitted by the Author:	06-Dec-2015
Complete List of Authors:	Xing, Hongzhu; Northeast Normal University, College of Chemistry; Liu, Yue; Northeast Normal University, College of Chemistry Chen, Dashu; Northeast Normal University, Faculty of Chemistry Li, Xingyu; Northeast Normal University, College of Chemistry Yu, Ziyang; Northeast Normal University, College of Chemistry Xia, Qiansu; Northeast Normal University, Department of Chemistry Liang, Desheng; Shenzhen EPT Battery Co., Ltd

Journal Name

ARTICLE

Visible-Light-Induced Controlled Radical Polymerization of Methacrylates Mediated by Pillared-Layer Metal-Organic Framework†

Received 00th January 20xx,
Accepted 00th January 20xx

DOI: 10.1039/x0xx00000x

www.rsc.org/

Yue Liu,‡[a] Dashu Chen,‡[a] Xingyu Li,[a] Ziyang Yu,[a] Qiansu Xia,[a] Desheng Liang[b] and Hongzhu Xing*,[a]

A novel visible light responsive metal-oragnic framework (MOF) with pillared-layer structure has been constructed from photoactive anthracene derived bipyridine. The as-prepared MOF was studied by single crystal X-ray diffraction, steady-state fluorescence, and electron paramagnetic resonance and so on. Studies reveal the visible light induced free radical formation of the bipyridine pillars in the MOF structure. Consequently, the promising photocatalytic reaction of atom transfer radical polymerization for methacrylates monomers was performed upon the utilization of the MOF material as photosensitizer to reduce the copper catalyst via electron transfer. It has been demonstrated that the reaction shows characteristics of controlled radical polymerization and the prepared polymers are of narrow molecular weight distributions and high retention of chain-end activities. Moreover, the photopolymerization can be easily manipulated by light switching.

1. Introduction

Metal-organic frameworks (MOFs) are solid-state hybrid compounds which are ideal candidate materials to address many enduring societal challenges involving energy and environmental sustainability.[1-5] These crystalline materials offer a high degree of tunability from structure and functionality, due largely to the target specific building blocks prior to the structure assembly.[6-10] Notable progress such as degradation of organic pollutants,[11,12] water splitting[13,14] and CO_2 reduction[15,16] has been made by photocatalysis of MOFs until now.[17] Even though some photoactive MOFs have been reported, the design and synthesis of visible light photoactive MOFs is still of great challenge. The pillared-layer method in which polycarboxylates act as layer-forming ligands and polypyridines act as pillars, has shown very high predictability to construct new MOFs with target specific functionality.[18-22] Successful examples including MOFs based on zinc dimer paddlewheel-like unit, with a range of pore sizes and even with built-in catalytic functionality have been described.[23-26] Whereas visible light responsive MOFs constructed by pillared-layer approach are rarely reported and the utilization of MOFs to catalyze useful organics transformation is still in a nascent but promising stage.

Controlled radical polymerization (CRP) techniques have revolutionized the field of polymer chemistry, allowing non-experts facile access to functionalized polymer materials with well-defined structure and architecture.[27-29] Among the various CRP techniques, atom transfer radical polymerization (ATRP) might be the most efficient method and it operates via a redox equilibrium process mediated by ligated metal catalysts.[30-38] More recently, photoinduced ATRP has been developed rapidly due to its unique feature of temporal and spatial control of chain extension process.[39-47] A fundamental element in this reaction is that the chain end is dormant in the absence of irradiation, but available for reactivation upon re-exposure to light. Notably, several semiconductor materials have recently been utilized to initiate the photoinduced ATRP where in situ generation of activator Cu(I) complex by reducing deactivator of Cu(II) complex was achieved in the reaction.[48,49] However, the utilization of MOFs for photoinduced polymerizations has rarely been studied. We are intrigued by the possibility of harnessing MOFs photoinduced redox reactivity for living polymerization. Our strategy is to introduce visible-light-induced redox property of MOFs materials by incorporation of photoactive organic chromophores in ligands. By application of the pillared-layer approach, we present here a new visible light photoactive MOFs material constructed from anthracene derived pillaring ligand. The as-prepared MOFs material shows intriguing long-lived photoinduced charge separation from bipyridine pillars. Remarkably, it can serve as efficient heterogeneous photosensitizer to initiate the ATRP reaction for the synthesis of polymethacrylate materials in a well-controlled way under visible light.

[a] Provincial Key Laboratory of Advanced Energy Materials, College of Chemistry, Northeast Normal University, Changchun, 130024, China
[b] Shenzhen EPT Battery Co., Ltd, Shenzhen, 518109, China
E-mail: xinghz223@nenu.edu.cn
‡Y. Liu and D. Chen contributed equally to this work.
†Electronic Supplementary Information (ESI) available. See DOI: 10.1039/x0xx00000x

2. Experimental section

2.1 Synthesis of NNU-35

The bipyridine pillar L_1 [9,10-bis(4'-pyridylethynyl)-anthracene] derived from anthracene was first prepared from 9,10-dibromoanthracene and 4-ethynylpyridine hydrochloride by Sonogashira coupling reaction (see the Supporting Information). Then the MOF compound, denoted as **NNU-35**, was synthesized using the solvothermal method. Typically, a mixture of $ZnCl_2$ (43 mg, 0.316 mmol), terephthalic acid (26 mg, 0.158 mmol), L_1 (30 mg, 0.079 mmol) and HCl (0.1 M, 10 μL) in N, N-dimethylformamide (DMF) (15 mL) was transferred into a glass vial placed at 85 °C for 36 h. Red crystals of **NNU-35** were collected and washed by ethanol for three times. IR (KBr, cm^{-1}): $\tilde{\upsilon}$ = 3057 (arom.CH), 2200 (C≡C), 1681, 1604-1437 (Ar), 823 (4-monosubst.Pyridine) (seeing Fig. S6, ESI†). The crystal data and structural refinement for **NNU-35** is shown in Table S1 (see the Supporting Information). CCDC 1410763 contains the supplementary crystallographic data for this paper. These data can be obtained free of charge from The Cambridge Crystallographic Data Centre via http://www.ccdc.cam.ac.uk/data_request/cif.

2.2 Characterization

Powder X-ray diffraction (PXRD) patterns were recorded on a Rigaku D-MAX 2550 radiation (λ = 0.15417 nm) with 2ϑ ranging from 3° to 40°. Thermogravimetric analyses (TGA) were carried out with the Perkin-Elmer TGA-7 thermogravimetric analyzer at a heating rate of 10 °C min^{-1} from room temperature to 800 °C under atmosphere. Solid state diffuse reflectance spectra (DRS) were taken on a HITACHI U-4100 spectrophotometer while the UV-Vis spectra for liquid sample were taken on a SHIMADZU UV-2550 spectrophotometer. The Fourier transform infrared (FTIR) spectra were recorded using KBr pellets in the range of 4000–400 cm^{-1} on a Mattson Alpha-Centauri spectrometer. Steady-state fluorescence spectra were measured on FLSP920 Edinburgh Fluorescence Spectrometer at room temperature. ^{1}HNMR spectra were recorded at 25 °C on a Varian 500 MHz. Electron paramagnetic resonance (EPR) spectra were obtained on a JES-FA 200 EPR spectrometer; scanning frequency: 9.45 GHz; central field: 340 mT; scanning width: 40 mT; scanning power: 0.998 mW; scanning temperature: 25 °C. The in suit experiments were carried out using a 500 W xenon arc lamp where a 420 nm optical filter was used to cut off ultraviolet part of light. The stable radical 2,2-diphenyl-1-picrylhydrazyl (DPPH) was used as a standard for the calculation of *g* values. Gel permeation chromatography (GPC) measurements were performed on Agilent Technologies PL-GPC-50 Integrated GPC system. THF was used as an eluent at flow rate of 1.0 mL min^{-1} at 30 °C. The molecular weights were calibrated with polymethyl methacrylate (PMMA) standards.

2.3 Photocatalytic ATRP reactions

Methacrylate monomers of methyl methacrylate (MMA, 99.8%), *n*-butyl methacrylate (*n*-BMA, 98%) and *i*-butyl methacrylate (*i*-BMA, 98%) were purified through an alumina column. The PMDETA is N,N,N',N'',N'''-pentamethyldiethylenetriamine and EBiB is ethyl α-bromoisobutyrate. A mixture of MMA monomers (2 mL, 18.6 mmol), PMDETA (11.6 μL, 0.056 mmol), $CuBr_2$ (4.1 mg, 0.019 mmol), EBiB (13 μL, 0.093 mmol) and **NNU-35** in acetonitrile (0.5 mL, 9.62 mmol) were placed in a Schlenk tube. The reaction mixture was degassed by freeze–pump–thaw cycles and left in vacuum. The mixture was irradiated by a xenon lamp equipped with band-pass optical mirror and filter, emitting light nominally at 520 nm at room temperature. The light intensity was 25 mW cm^{-2} measured by Delta Ohm model HD-9021 radiometer. The resulted polymers were precipitated in methanol and then dried in vacuum. Chain extension experiment was performed with a macroinitiator of PMMA-Br prepared as above, instead of EBiB. The polymerization conditions for *n*-BMA and *i*-BMA were the same as that of MMA.

3. Results and discussion

Single-crystal X-ray diffraction measurement manifests that **NNU-35** crystallizes in the monoclinic space group *C*2/*c* with a formula of $[Zn(bdc)(L_1)]_2 \cdot DMF$. The compound is featured by the pillared-layer structure in which the layers are constructed from zinc ions bridged by the terephthalate ligand and these layers are pillared by the anthracene bipyridine (Fig. 1a). A "two-blade paddlewheel" building unit of zinc dimer ($Zn_2O_8N_4$) is formed where the zinc atoms are both in distorted octahedral geometry coordinated by one chelating carboxylate group, two oxygen atoms from bidentate bridging terephthalate ligands, and two nitrogen atoms from the bipyridine pillars (Fig. S1a, ESI†). Such two-blade paddlewheel coordination of metallic dimer has also been observed in other pillared MOFs.[50-53] Owing to the different coordination modes of the terephthalates, distorted 4 × 4 grid was constructed from the two-blade paddlewheel dimeric unit, forming the two dimensional layer in the structure (Fig. 1b). It is worth to mention that, different from the square paddlewheel $Zn_2O_8N_4$ building units, the two-blade paddlewheel unit coordinates to pillaring ligand in pairs (Fig. 1c), constructing the desired pillared-layer network. Naturally, π-conjugated interaction between pillar-pillar pairs is observed where the face to face distance between pillars is about 3.4 Å. It is well known that the tendency to interpenetrate in MOFs is high when the connectors are long, as is the case here, there are two independent networks which are interpenetrated by each other (Fig. S1b, ESI†). Given that the layers are pillared by anthracene-based bipyridine ligand in pairs, which strengthens the coordination interaction between the layers, one may regard the structure to have low flexibility. The thermal gravimetric analysis shows that the neutral framework is thermal stable up to 350 °C with removal of guest molecule of DMF (Fig. S2, ESI†). The powder X-ray diffraction pattern matches well with the simulated one from crystal structure, indicative of pure phase of the as-prepared bulk material (Fig. S3, ESI†).

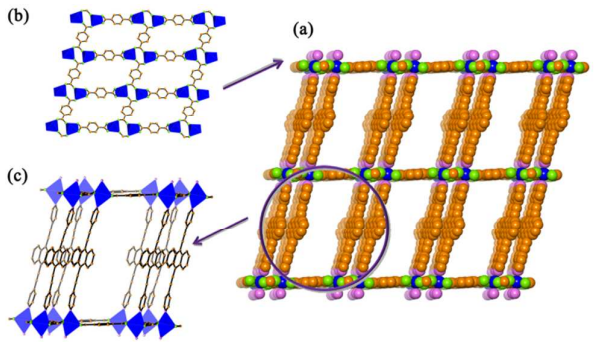

Fig. 1 (a) The pillared-layer framework of **NNU-35**; (b) The layer constructed by terephthalic acid and zinc dimer; (c) A view showing the in-pair pillars. Blue, green, pink, and orange spheres/polyhedra represent zinc, oxygen, nitrogen and carbon atoms, respectively. All hydrogen atoms and guest molecules are omitted for clarity.

The UV-vis absorption of **NNU-35** was first studied with crystalline sample at room temperature (Fig. 2a). **NNU-35** shows a broad absorption band in the visible light region with absorption edge at about 650 nm. As compared with anthracene-based ligand L_1, the absorption of **NNU-35** expands to low energy region. The broad absorption band of **NNU-35** is attributed to inhomogeneous broadening which arises from energy transfer and/or charge transfer interactions in the structure,[54-56] which is further proved by the steady-state fluorescence spectra. As shown in Fig. 2b, different from the characteristic yellow-green fluorescence of anthracene based ligand centered at 480 and 510 nm and its corresponding weak emission in solid state (about 590 nm) due to the abundant conjugation interactions, **NNU-35** exhibits broad emission band centered at 680 nm. Such a significant red shift of fluorescence should result primarily from the ligand-metal charge transfer (LMCT) interaction in the structure, which is not uncommon in the MOFs structures.[54,56]

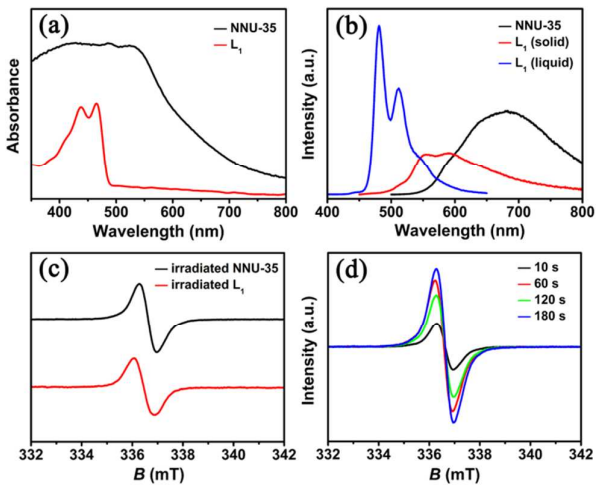

Fig. 2 (a) UV–vis absorption spectra of **NNU-35** and anthracene-based pillar (L_1); (b) Fluorescence spectra of **NNU-35** and L_1 (liquid and solid); (c) EPR spectra of **NNU-35** and L_1 upon light irradiation; (d) Time-evolution EPR signals for **NNU-35** under in situ visible light illumination.

EPR spectroscopy usually provides valuable information for photoinduced charge generation following the excitation.[57] The as-prepared crystalline sample of **NNU-35** was first studied by EPR and it displayed no obvious EPR signal, whereas, a sharp and narrow EPR signal at g = 2.003 was detected when the MOF sample had been exposed to visible light, and the same signal was also observed for the bipyridine pillar L_1 (Fig. 2c). This resonance sustained about several minutes even without light irradiation, suggesting clearly its free radical nature. The photoinduced charge generation in **NNU-35** is further demonstrated by time-evolution EPR experiments. The time-evolution measurements were performed where visible light excitation was done in situ using xenon lamp. As expected, the intensity of EPR resonance at g = 2.003 increased obviously upon visible light irradiation and reached a maximum at about 3 minute under continuous illumination (Fig. 2d). The same time-evolution measurements were also conducted for the bipyridine pillar and identical results were obtained (Fig. S4, ESI†). Hence it is clear that the formation of free radicals in **NNU-35** is from the bipyridine pillar ligand.

In order to take advantage of the broad visible light absorption and desirable charge separation in **NNU-35**, a useful and promising photocatalytic system of ATRP reaction for polymer synthesis was designed where the as-prepared **NNU-35** serves as photosensitizer for the reduction of copper complex. Typical ATRP reaction system of MMA with $[MMA]_o/[EBiB]_o/[CuBr_2]_o/[PMDETA]_o$ = 200/1/0.2/0.6 was chosen where the copper complex is catalyst and EBiB is the initiator. To avoid the confusion caused by absorption of the Cu(II)/PMDETA complex, the reaction was first studied by UV-vis spectra. As shown in Fig. S5 ESI†, the reaction mixture displayed an almost transparent region from 500 to 600 nm in the spectrum, whereas **NNU-35** shows a strong absorption in this region (Fig. 2a). Therefore the following photoinduced ATRP reactions were performed under the monochromatic light at 520 nm. A control experiment at this wavelength showed that the reaction did not conduct in the absence of **NNU-35** (Table 1, entry 1).

Upon the addition of **NNU-35**, the visible light photoinduced reaction polymerized 48% monomer after 8 h irradiation where a reletively narrow moelcular weight distribution (M_w/M_n) of 1.12 was oberserved (entry 2). This result suggests the feasibility of the as supposed photocatalytic system. As shown in Table 1, to understand the role of other components except photoactive MOF, a range of experiments involving the absense of EBiB, PMDETA and $CuBr_2$ were conducted. Results show that EBiB and PMDETA are both essential for the photoinduced ATRP reaction where no polymer was produced in the absense of them (entries 3 and 4). In contrast, the polymerization without $CuBr_2$ (entry 5) was out of control showing extra large molecular weight ($M_{n,GPC}$ = 195800) and wide molecular weight distribution (M_w/M_n = 2.11). This phenomenon can be reasoned by the direct initiation of the reaction, resulting from the classical halogen abstraction between the EBiB initiator and oxidizing radical cation of bipyridine pillar.[58] Considering the heterogeneous nature of **NNU-35** in the reaction, its infulence should be investigated.

Journal Name

ARTICLE

Table 1 The results of photoinduced ATRP using **NNU-35** as photocatalyst

Entry[a)]	$[MMA]_0/[EBiB]_0$ $/[CuBr_2]_0/[PMDETA]_0$	NNU-35 (mg)	Monomer	Conversion [%]	$M_{n,th}$[b)] [g mol^{-1}]	$M_{n,GPC}$[c)] [g mol^{-1}]	M_w/M_n[c)]
1	200/1/0.2/0.6	-	MMA	-	-	-	-
2	200/1/0.2/0.6	20	MMA	48	9600	20500	1.12
3	200/0/0.2/0.6	20	MMA	-	-	-	-
4	200/1/0.2/0	20	MMA	-	-	-	-
5	200/1/0/0.6	20	MMA	25	5100	195800	2.11
6	200/1/0.2/0.6	10	MMA	45	9000	19700	1.16
7	200/1/0.2/0.6	30	MMA	52	10400	20300	1.18
8	200/1/0.1/0.3	20	MMA	21	9400	19500	1.15
9	200/1/0.05/0.15	20	MMA	19	10700	21200	1.29
10	200/1/0.2/0.6	20	*n*-BMA	57	16200	24900	1.19
11	200/1/0.2/0.6	20	*i*-BMA	50	14200	24500	1.20
12[d)]	200/1/0.2/0.6	20	St	25	5200	15100	1.15

[a)] Irradiation time = 8 h, irradiation wavelegth = 520 nm; [b)] $M_{n,th} = [MMA]_0/[EBiB]_0 \times M_{w,mon} \times$conversion; [c)] Number-average molecular weight ($M_{n,GPC}$) and molecular-weight distribution (M_w/M_n) were determined by GPC; [d)] The initiator of EtBP (ethyl 2-bromopropionate), instead of EBiB, is used for the polymerization of styrene (St).

Experiments showed that polymers with moderate monomer conversion (45%–52%) and narrow molecular wight distibution (M_w/M_n = 1.12–1.18) were obtained when the dosage of **NNU-35** was in the range of 10–30 mg (entries 6 and 7). Moreover, decreasing the Cu(II)/PMDETA amount to lower concentrations resulted in slower polymerization with low monomer conversion (ca. 20%), while acceptable narrow molecular weight distribution was perserved (entries 8 and 9).

The versatility of the system was studied for polymerization of other vinyl monomers such as *n*-BMA and *i*-BMA in entries 10 and 11. For both monomers, the polymerization was successfully carried out with narrow molecular weight distributions and good conversions of 57% (*n*-BMA) and 50% (*i*-BMA), respectively. It is notable that the reaction shows selectivity for monomers when EBiB is used as initiator. Experiments showed that the polymerizations for monomers such as styrene and vinyl acetates were not succeeded; whereas the polymerization of styrene was observed when another initiator of EtBP (ethyl 2-bromopropionate) was used instead of EBiB (entry 12).

The kinetic plot of the photoinduced ATRP and the evolution of molecular weight together with distribution upon monomer conversion were investigated for the photopolymerization of MMA (Fig. 3a and 3b). At first, the photopolymerization exhibited an induction period of about three hours during which the monomer conversion was very low and no polymer was obtained. After the induction period, polymerization was rapid and followed first-order kinetics, indicative of controlled radical polymerization where the propagating radical concentration is almost constant. During the process of photopolymerization, the experimental molecular weights ($M_{n,GPC}$) are larger than those calculated theoretically ($M_{n,th}$) but the molecular weight dispersities (M_w/M_n) are almost constant. This result is likely due to the slow initiation when EBiB was used as initiator. It is well-known that dimethyl 2-bromo-2,4,4-trimethylglutarate, formed after reaction of EBiB with one molecule of MMA, can be considered as a model for dimeric initiator which initiates the reaction faster than the original initiator of EBiB.[47,59]

The living character of the reaction was demonstrated by chain extention experiment with the as-prepared polymer of PMMA-Br as macroinitiator, instead of EBiB. The PMMA-Br macroinitiator (M_n = 10600 g mol^{-1} with M_w/M_n = 1.09) was first prepared by this photoATRP. Chain extension experiment was then performed under identical experimental conditions with $[MMA]_0/[PMMA\text{-}Br]_0/[CuBr_2]_0/[PMDETA]_0$ ratio of 200/0.1/0.2/0.6 for 4h. Gel-permeation chromatography (GPC) measurment showed that the chain-extended PMMA with M_n = 62000 g mol^{-1} and M_w/M_n = 1.17 was obtained without detectable unreacted macroinitiator (Fig. 3c). This experiment provides that a good control over the chain-growth process can be easily realized.

One of the advances of ATRP induced by photon relys on triggering the reaction easily through light switching. To illustrate this, the visible light was periodically turned on and off (Fig. 3d). No polymerization has taken place when the the reaction was placed in the dark for 4h. After that, the reaction was exposed to light (520 nm), reaching 16.6% conversion of monomer in 4h. And then, the light was turned-off where no obvious monomer conversion was observed during the course of 4h, indicating a negligible concentration of the active radical without light irradiation.

Consequently, reexposure to 520 nm light led to further progress of the reaction. Such cycle could be repeated for further experiment upto higher conversion of ~60%. Hence it is clearly demonstrated that the **NNU-35** mediated ATRP could be easily contolled by light.

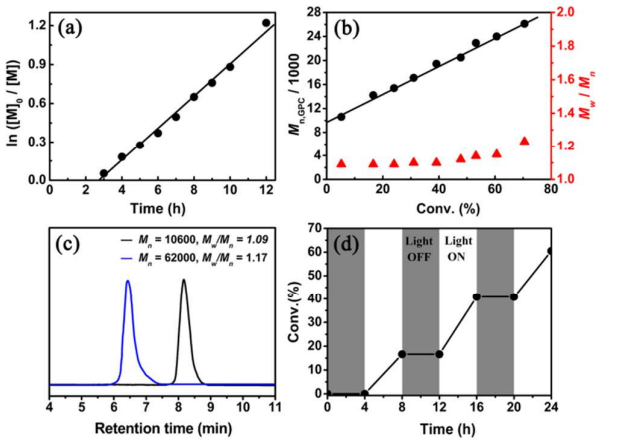

Fig. 3 (a) Kinetic plots; (b) Evolution of the molar mass and M_w/M_n upon conversion of MMA during photoinduced ATRP; (c) GPC analysis of the samples before (black line) and after (blue line) the chain extension process; (d) Photoregulating effect of the polymerization of MMA mediated by **NNU-35**. Conditions for (a), (b) and (d): $[MMA]_0/[EBiB]_0/[CuBr_2]_0/[PMDETA]_0$ = 200/1/0.2/0.6 in 2mL acetonitrile, **NNU-35** = 20 mg. Condition for (c): $[MMA]_0/[PMMA\text{-}Br]_0/[CuBr_2]_0/[PMDETA]_0$ = 200/0.1/0.2/0.6 in in 2mL acetonitrile for 4 h, **NNU-35** = 20 mg. All reactions were carried out at room temperature using 520 nm visible light.

The **NNU-35** mediated polymerization relys on continuous regeneration of copper catalyst by electron transfer (AGET) ATRP mechanism. A plausible mechanism for this two-component photocatalytic system is illustrated in Scheme 1, where the oxidized Cu(II)/PMDETA complex is reduced by heterogeneous MOF photosensitizer of **NNU-35** via single electron transfer, the resulting Cu(I) complex reacts with initiator of alkyl halide (R-X) forming radicals (R•) to initiate the ATRP. Meanwhile, the positive "hole" of ligand radical in **NNU-35** oxidizes the reductive amine to retain its pristine structure, whereafter the reaction intermediate amine$^+$X$^-$ supports the chain-end halogen for the dormant species and returns to amine.[60] Moreover, the heterogeneous **NNU-35** is easily recovered by centrifugation. As evidenced by PXRD study, the structure of **NNU-35** was maintained after ATRP reaction, allowing its reuse in the subsequent reactions (Fig. S3, ESI†). The recycle experiments demonstrated that **NNU-35** can be reused at least three times showing almost identical activity (Fig. S7, ESI†). Despite the success of **NNU-35** to initiate the photoinduced ATRP, the reaction suffers from low conversion. This should be primarily due to that the reaction is carried out at room temperature. It is well known that the activation energy for the radical propagation is usually higher than that for the radical termination. Therefore the polymerization rate and the conversion in ATRP increase with increasing temperature due to the augment of both the radical propagation rate constant and the atom transfer equilibrium constant, vice versa, the reaction at low temperature needs longer time showing lower conversion.[61] Besides, the use of copper complex in the reaction is not enviroment friendly. Our ongoing work is to initiate the polymerization by direct photoinduced charge transfer (PET) from MOF to initiator moleucle, eliminating the use of transition metal complex.

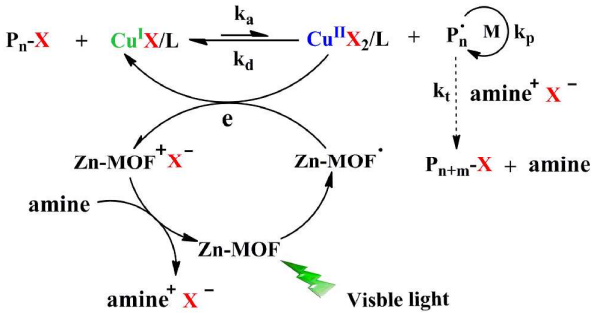

Scheme 1. Proposed mechanism for **NNU-35** mediated ATRP under visible light.

4. Conclusions

In summary, a novel visible light responsive MOFs material **NNU-35** has been constructed from photoactive anthracene-derived bipyridine ligand by pillaring-layer method. The desirable long-lived charge separation has been achieved in **NNU-35**. Studies reveal that the photoinduced charge separation relys on free radical formation of anthracene-based ligand. Consequently, the promising photocatalytic reaction of ATRP for useful polymer synthesis was performed upon the utilization of photoactive **NNU-35** as photosensitizer to reduce the copper catalyst via electron transfer. Results show that the polymerization of methacrylate monomers was easily contolled exihibiting chatacters of living radical polymerization. The resulting polymers are of narrow molecular weight distribution and high retention of chain-end activity. Additionaly, the reaction can be easily manipulated by light switching. The success of **NNU-35** for ATRP reaction has expanded the usage of photoactive MOFs into polymer synthesis. It is also demonstrated here that the design and preparation of MOFs photocatalysts by photoactive organic ligand is a feasible method.

Acknowledgements

This work is supported by the National Natural Science Foundation of China (21473024 and 21101023) and Natural Science Foundation of Jilin Province (20140101228JC).

References

1 O. K. Farha and J. T. Hupp, *Acc. Chem. Res.*, 2010, **43**, 1166–1175.

2 S. Kitagawa, R. Kitaura and S. Noro, *Angew. Chem. Int. Ed.*, 2004, **43**, 2334–2375.
3 S.-L. Li and Q. Xu, *Energy Environ. Sci.*, 2013, **6**, 1656–1683.
4 S. T. Meek, J. A. Greathouse and M. D. Allendorf, *Adv. Mater.*, 2011, **23**, 249–267.
5 O. M. Yaghi, M. O'Keeffe, N. W. Ockwig, H. K. Chae, M. Eddaoudi and J. Kim, *Nature*, 2003, **423**, 705–714.
6 T. R. Cook, Y. R. Zheng and P. J. Stang, *Chem. Rev.*, 2013, **113**, 734–777.
7 M. Eddaoudi, J. Kim, N. Rosi, D. Vodak, J. Wachter, M. O'Keeffe and O. M. Yaghi, *Science*, 2002, **295**, 469–472.
8 V. Guillerm, D. Kim, J. F. Eubank, R. Luebke, X. Liu, K. Adil, M. S. Lah and M. Eddaoudi, *Chem. Soc. Rev.*, 2014, **43**, 6141–6172.
9 Y. He, B. Li, M. O'Keeffe and B. Chen, *Chem. Soc. Rev.*, 2014, **43**, 5618–5656.
10 W. Lu, Z. Wei, Z. Y. Gu, T. F. Liu, J. Park, J. Park, J. Tian, M. Zhang, Q. Zhang, T. Gentle, 3rd, M. Bosch and H. C. Zhou, *Chem. Soc. Rev.*, 2014, **43**, 5561–5593.
11 Y. L. Hou, R. W. Sun, X. P. Zhou, J. H. Wang and D. Li, *Chem. Commun.*, 2014, **50**, 2295–2297.
12 K. G. M. Laurier, F. Vermoortele, R. Ameloot, D. E. De Vos, J. Hofkens and M. B. J. Roeffaers, *J. Am. Chem. Soc.*, 2013, **135**, 14488–14491.
13 P. Du and R. Eisenberg, *Energy Environ. Sci.*, 2012, **5**, 6012–6021.
14 J.-L. Wang, C. Wang and W. Lin, *ACS Catal.*, 2012, **2**, 2630–2640.
15 Y. Fu, D. Sun, Y. Chen, R. Huang, Z. Ding, X. Fu and Z. Li, *Angew. Chem. Int. Ed.*, 2012, **51**, 3364–3367.
16 S. Wang, W. Yao, J. Lin, Z. Ding and X. Wang, *Angew. Chem. Int. Ed.*, 2014, **53**, 1034–1038.
17 T. Zhang and W. Lin, *Chem. Soc. Rev.*, 2014, **43**, 5982–5993.
18 B. J. Burnett, P. M. Barron, C. Hu and W. Choe, *J. Am. Chem. Soc.*, 2011, **133**, 9984–9987.
19 J. F. Eubank, L. Wojtas, M. R. Hight, T. Bousquet, V. Kravtsov and M. Eddaoudi, *J. Am. Chem. Soc.*, 2011, **133**, 17532–17535.
20 S. Henke, A. Schneemann, A. Wutscher and R. A. Fischer, *J. Am. Chem. Soc.*, 2012, **134**, 9464–9474.
21 P. Kanoo, G. Mostafa, R. Matsuda, S. Kitagawa and T. K. Maji, *Chem. Commun.*, 2011, **47**, 8106–8108.
22 X. F. Wang, Y. Wang, Y. B. Zhang, W. Xue, J. P. Zhang and X. M. Chen, *Chem. Commun.*, 2012, **48**, 133–135.
23 S. Jin, H. J. Son, O. K. Farha, G. P. Wiederrecht and J. T. Hupp, *J. Am. Chem. Soc.*, 2013, **135**, 955–958.
24 C. Y. Lee, O. K. Farha, B. J. Hong, A. A. Sarjeant, S. T. Nguyen and J. T. Hupp, *J. Am. Chem. Soc.*, 2011, **133**, 15858–15861.
25 M. C. So, S. Jin, H. J. Son, G. P. Wiederrecht, O. K. Farha and J. T. Hupp, *J. Am. Chem. Soc.*, 2013, **135**, 15698–15701.
26 H. J. Son, S. Jin, S. Patwardhan, S. J. Wezenberg, N. C. Jeong, M. So, C. E. Wilmer, A. A. Sarjeant, G. C. Schatz, R. Q. Snurr, O. K. Farha, G. P. Wiederrecht and J. T. Hupp, *J. Am. Chem. Soc.*, 2013, **135**, 862–869.
27 W. A. Braunecker and K. Matyjaszewski, *Prog. Polym. Sci.*, 2007, **32**, 93–146.
28 J. Nicolas, Y. Guillaneuf, C. Lefay, D. Bertin, D. Gigmes and B. Charleux, *Prog. Polym. Sci.*, 2013, **38**, 63–235.
29 M. Ouchi, T. Terashima and M. Sawamoto, *Chem. Rev.*, 2009, **109**, 4963–5050.
30 L. E. N. Allan, M. R. Perry and M. P. Shaver, *Prog. Polym. Sci.*, 2012, **37**, 127–156.
31 A. Gregory and M. H. Stenzel, *Prog. Polym. Sci.*, 2012, **37**, 38–105.
32 Y. Guillaneuf, D. L. Versace, D. Bertin, J. Lalevee, D. Gigmes and J. P. Fouassier, *Macromol. Rapid Commun.*, 2010, **31**, 1909–1913.
33 C. J. Hawker, A. W. Bosman and E. Harth, *Chem. Rev.*, 2001, **101**, 3661–3688.
34 D. J. Keddie, G. Moad, E. Rizzardo and S. H. Thang, *Macromolecules*, 2012, **45**, 5321–5342.
35 K. Matyjaszewski, *Macromolecules*, 2012, **45**, 4015–4039.
36 K. Matyjaszewski, S. Gaynor and J.-S. Wang, *Macromolecules*, 1995, **28**, 2093–2095.
37 R. Poli, *Angew. Chem. Int. Ed.*, 2006, **45**, 5058–5070.
38 D. J. Siegwart, J. K. Oh and K. Matyjaszewski, *Prog. Polym. Sci.*, 2012, **37**, 18–37.
39 B. P. Fors and C. J. Hawker, *Angew. Chem. Int. Ed.*, 2012, **51**, 8850–8853.
40 A. Ohtsuki, L. Lei, M. Tanishima, A. Goto and H. Kaji, *J. Am. Chem. Soc.*, 2015, **137**, 5610–5617.
41 X. Pan, M. Lamson, J. Yan and K. Matyjaszewski, *ACS Macro Lett.*, 2015, **4**, 192–196.
42 A. J. Perkowski, W. You and D. A. Nicewicz, *J. Am. Chem. Soc.*, 2015, **137**, 7580–7583.
43 N. J. Treat, B. P. Fors, J. W. Kramer, M. Christianson, C.-Y. Chiu, J. R. d. Alaniz and C. J. Hawker, *ACS Macro Lett.*, 2014, **3**, 580–584.
44 A. Ohtsuki, A. Goto and H. Kaji, *Macromolecules*, 2013, **46**, 96–102.
45 Y. Kwak and K. Matyjaszewski, *Macromolecules,* 2010, **43**, 5180–5183.
46 M. A. Tasdelen, M. Uygun and Y. Yagci, *Macromol. Rapid Commun.*, 2011, **32**, 58–62.
47 J. Mosnáček and M. Ilčíková, *Macromolecules*, 2012, **45**, 5859–5865.
48 S. Dadashi-Silab, M. Atilla Tasdelen, A. Mohamed Asiri, S. Bahadar Khan and Y. Yagci, *Macromol. Rapid Commun.*, 2014, **35**, 454–459.
49 S. Dadashi-Silab, M. A. Tasdelen, B. Kiskan, X. Wang, M. Antonietti and Y. Yagci, *Macromol. Chem. Phys.*, 2014, **215**, 675–681.
50 J. Tao, M.-L. Tong and X.-M. Chen, *J. Chem. Soc., Dalton Trans.*, 2000, 3669–3674.
51 T. Yamada, S. Iwakiri, T. Hara, K. Kanaizuka, M. Kurmoo and H. Kitagawa, *Cryst. Growth Des.*, 2011, **11**, 1798–1806.
52 T. Yamada and H. Kitagawa, *J. Am. Chem. Soc.*, 2009, **131**, 6312–6313.
53 B. Zheng, J. Luo, F. Wang, Y. Peng, G. Li, Q. Huo and Y. Liu, *Cryst. Growth Des.*, 2013, **13**, 1033–1044.
54 S. Bordiga, C. Lamberti, G. Ricchiardi, L. Regli, F. Bonino, A. Damin, K. P. Lillerud, M. Bjorgen and A. Zecchina, *Chem. Commun.*, 2004, 2300–2301.
55 M. Ji, X. Lan, Z. Han, C. Hao and J. Qiu, *Inorg. Chem.*, 2012, **51**, 12389–12394.
56 G. Zhang, G. Kim and W. Choi, *Energy Environ. Sci.*, 2014, **7**, 954–966.
57 J. Long, S. Wang, Z. Ding, S. Wang, Y. Zhou, L. Huang and X. Wang, *Chem. Commun.*, 2012, **48**, 11656–11658.
58 M. Ciftci, M. A. Tasdelen and Y. Yagci, *Polym. Chem.*, 2014, **5**, 600–606.
59 T. Ando, M. Kamigaito and M. Sawamoto, *Tetrahedron*, 1997, **53**, 15445–15457.
60 S. Shanmugam, J. Xu and C. Boyer, *J. Am. Chem. Soc.*, 2015, **137**, 9174–9185.
61 K. Matyjaszewski and J. Xia, *Chem. Rev.,* 2001, **101**, 2921–2990.

Graphic Abstract

A visible light responsive MOFs material has been constructed by the pillared-layer approach to conduct atom transfer radical polymerization, where the photo polymerization shows characteristics of living polymerization and the as-prepared polymers are of narrow molecular weight distribution and high retention of chain-end activity.